[6] The dimensions of the grid are defined as the distances between the metal atoms separated by **1**.
[7] The interlayer separation is defined as the distance of the Ni atoms to the plane of the neighboring layer.
[8] The diffraction pattern of **3** does not exactly match with the pattern that is calculated from its single-crystal data. This mismatch in X-ray powder diffraction patterns could be caused by incomplete conversion from mode A into mode B and hence **3** may also contain some impurity in the form of mode A packing.
[9] Crystallographic information for interpenetrated network: This structure was solved in two space groups: $I41/a$, $a = b = 19.276(3)$; $c = 28.942(9)$ Å; $\alpha = \beta = \gamma = 90°$ and $C2/c$, $a = 27.257(5)$; $b = 28.942(9)$; $c = 19.275(4)$ Å; $\beta = 134.992(4)°$. The solvent molecules are highly disordered.
[10] Styrene, nitrobenzene, and cyanobenzene were also found to exchange *o*-xylene in **2** in the same way as mesitylene.
[11] Preliminary results on **3**, from which the mesitylene was removed, indicate that it shows sorption properties with gaseous benzene.

Amplified DNA Detection by Electrogenerated Biochemiluminescence and by the Catalyzed Precipitation of an Insoluble Product on Electrodes in the Presence of the Doxorubicin Intercalator**

Fernando Patolsky, Eugenii Katz, and Itamar Willner*

The amplified sensing of nucleic acids on surfaces attracts research efforts directed to the development of DNA chips for gene analysis, the detection of genetic disorders, tissue matching, forensic applications, and molecular computation.[1,2] Amplified electrochemical DNA detection was reported by the labeling of nucleic acids with a redox enzyme and amplifying the formation of the double-stranded system on the electrode surface by the activation of a secondary bioelectrocatalyzed process.[3] A further approach involves the generation, on the electrode surface, of a redox-active replica for the analyzed DNA by using polymerase, and the application of the redox replica as a mediator for the activation of bioelectrocatalyzed transformations.[4] A different approach for the amplified detection of DNA includes the labeling of the analyzed DNA, for example, with a biotin label, that allows the secondary association of an enzyme conjugate (e.g. avidin–alkaline phosphatase or avidin–horseradish peroxidase) that stimulates the biocatalyzed precipitation of an insoluble product on the electrodes.[5,6] Faradaic impedance spectroscopy, which probes the interfacial electron-transfer resistance at the electrode supports, or microgravimetric quartz-crystal-microbalance (QCM) measurements were used as transduction methods for the accumulation of the insoluble products on the respective surfaces, as a result of the primary DNA-recognition events. Alternative methods to amplify DNA-recognition processes include the use of particulate labels, such as liposomes,[7] Au nanoparticles,[8] or CdS nanoparticles[9] as amplifying agents, and the electrochemical, microgravimetric QCM assay, and photoelectrochemical transduction of the DNA detection.

Electrogenerated chemiluminescence is a rapidly progressing method to image biosensing events on surfaces.[10,11] Studies pioneered by Bard and colleagues have employed Ru^{II}–polypyridine complexes that bind to a double-stranded (ds) DNA for the electroluminescent imaging of DNA on electrode surfaces.[12] However, the partial binding of $[Ru(bpy)_3]^{2+}$ (bpy = 2,2′-bipyridine) complexes to single-stranded DNA introduces significant background electroluminescence that prohibits the detection of low hybridization yields of DNA. The covalent labeling of nucleic acids with a Ru^{II}–trisbipyridine complex has been suggested as a possible route to resolve this difficulty.[13] Herein we report two alternative methods for the amplified detection of DNA by using the doxorubicin intercalator as a ds DNA surface-confined label for the electrogeneration of H_2O_2. The generated H_2O_2 is then used to image the DNA by: 1) stimulated biochemiluminescence, and 2) stimulated biocatalyzed precipitation of an insoluble product on electrodes.

Figure 1 depicts the configuration of the DNA detection system. The thiolated nucleic acid **1** is assembled on an Au-electrode and the surface coverage derived from the microgravimetric (QCM) analysis[7c] is 2×10^{-11} mol cm^{-2}. Then the **1**-functionalized gold surface is treated with 1-mercaptohexanol to block pinholes in the DNA-monolayer assembly associated with the electrode. The resulting monolayer-functionalized electrode is then treated with the complementary analyte-DNA **2**, to yield the ds DNA assembly on the electrode surface. The resulting system is further treated with doxorubicin (**3**), which is a specific intercalator in double-stranded CG base-pair-containing DNA sequences.[14] The intercalator-stimulated amplified analysis of the nucleic acid **2** is outlined in Figure 2. Electrochemical reduction of the intercalated **3** leads to the electrocatalyzed reduction of O_2 to H_2O_2. The electrogenerated H_2O_2 in the presence of luminol and horseradish peroxidase (HRP) leads to the formation of 3-aminophthalate and biochemiluminescence ($\lambda = 425$ nm)[10] which indicates the DNA hybridization process (Figure 2A). Alternatively, the electrogenerated H_2O_2 mediates in the presence of HRP the oxidation of 4-chloronaphthol (**4**) to the insoluble product **5**, which precipitates on the electrode.[15] Precipitation of **5** on the electrode insulates the electrode surface and increases its interfacial electron-transfer resistance. The changes in the interfacial electron-transfer resistances can then be followed in the presence of an electrolyte-soluble redox probe, by using Faradaic impedance spectroscopy. The stimulated light emission, or the biocatalyzed precipitation of **5** occurs only if the ds DNA structure with the

[*] Prof. I. Willner, F. Patolsky, Dr. E. Katz
Institute of Chemistry
The Farkas Center for Light-Induced Processes
The Hebrew University of Jerusalem
Jerusalem 91904 (Israel)
Fax: (+972) 2-6527715
E-mail: willnea@vms.huji.ac.il

[**] This research is supported by the German–Israeli Program (DIP). The Max Planck Award for International Cooperation (I.W.) is gratefully acknowledged.

Supporting information for this article is available on the WWW under http://www.angewandte.org or from the author.

  0044-8249/02/4118-3398 $ 20.00+.50/0

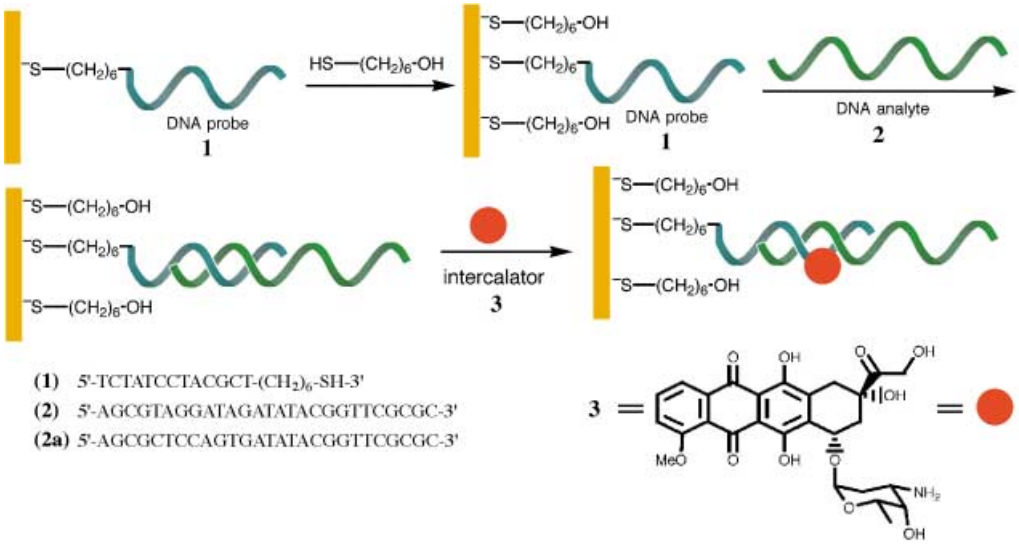

Figure 1. Assembly of the ds DNA monolayer with the intercalated doxorubicin molecules.

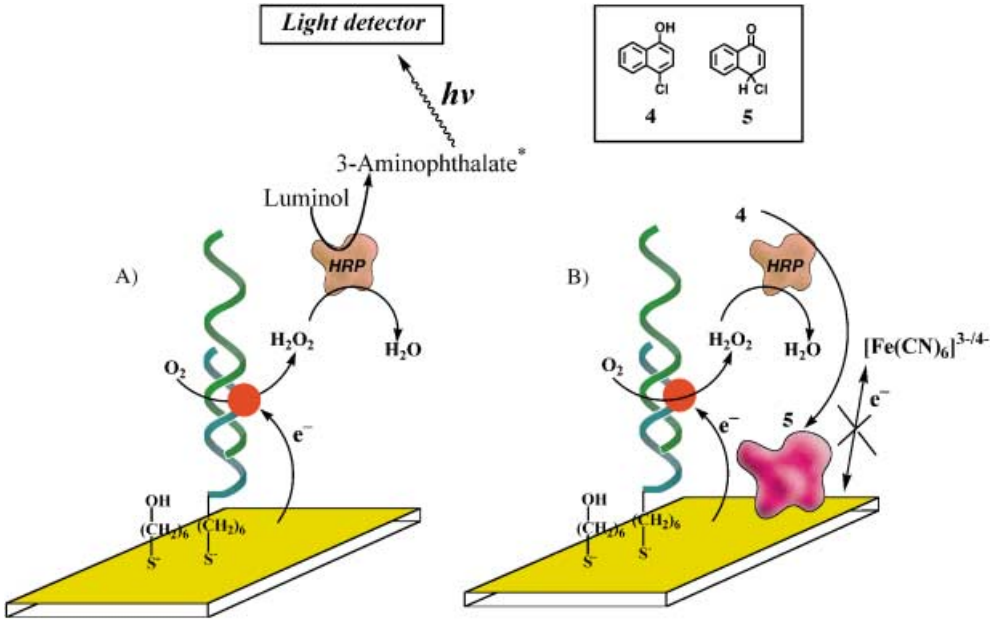

Figure 2. Amplified detection of DNA by the intercalated **3** using: A) Electrochemically generated biochemiluminescence. B) Electrochemically induced precipitation of an insoluble product on the electrode.

analyte nucleic acid **2** is formed, and provided that **3** binds to the assembly.

Figure 3 A, curve a, shows the differential pulse voltammogram of **3**, $E^{o} = -0.68$ V, which is intercalated in the ds DNA assembly formed between the **1**-functionalized monolayer-electrode and **2**. Figure 3 A, inset, shows the cyclic voltammogram of the intercalated **3**. Coulometric assay of the reduction wave of **3** indicates a surface coverage of **3** of 3×10^{-11} mol cm^{-2}. As the surface coverage of the double-stranded structures[16] of **1**/**2** is 8×10^{-12} mol cm^{-2}, we estimate that an average loading of a ds-DNA assembly with 3.75 units of **3** takes place. No redox response of **3** is observed when the single stranded **1**-monolayer is treated with the intercalator in a control experiment, Figure 3 A, curve b. Figure 3 B, curves a and b, show the cyclic voltammograms of the **1**- and **1**/**2**-monolayer-functionalized electrodes, respectively, after treatment with **3** under argon. The two systems reveal almost identical responses and the redox activity of **3**, which is expected to be observed for the **1**/**2**-assembly accommodating the intercalator, is almost invisible at the slow potential scan rate employed in the experiment. Figure 3 B, curve c, shows the electrical response of the **1**-functionalized electrode under oxygen. A cathodic current resulting from the non-catalytic reduction of O_2 is observed. Note that the generation of a densely packed, pinhole-free, monolayer of **1**/1-mercaptohexanol on the electrode surface is important to introduce a barrier and a high overpotential for the direct electroreduction of O_2. Figure 3 B, curve d, depicts the cyclic voltammogram of the **1**/**2**-functionalized electrode after the intercalation of **3** in the ds-DNA assembly in the presence of oxygen. The cathodic current originating from the quinone-intercalator-catalyzed reduction of O_2 is enhanced and the over-

  0044-8249/02/4118-3399 $ 20.00+.50/0

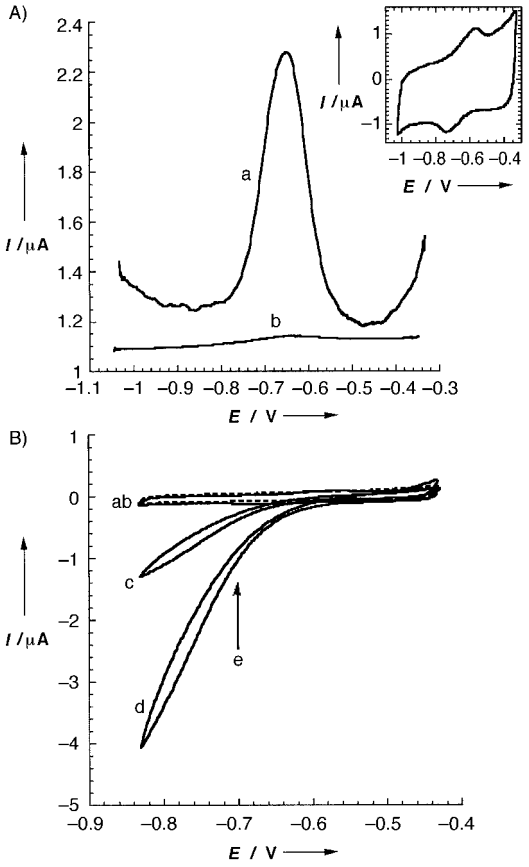

Figure 3. A) Differential pulse voltammograms of the Au-electrode functionalized with: a) the **1**/**2**-assembly and the intercalated **3**; b) The **1**-modified electrode treated with **3**, 5.2×10^{-5} M, and subsequently washed with phosphate buffer, pH 7.4. Potential scan rate, 20 mV s^{-1}; pulse height, 2 mV. Inset: Cyclic voltammogram of the **1**/**2**- and intercalator **3**-modified electrode. Potential scan rate, 100 mV s^{-1}. The data were recorded in 0.1 phosphate buffer, pH 7.0, under Ar. B) Cyclic voltammograms of the **1**-functionalized electrode after treatment with **3**: a) under Ar and c) in the presence of O_2. Cyclic voltammograms of **1**/**2**-functionalized electrode after treatment with **3**: b) under Ar and d) in the presence of O_2. Potential scan rate, 10 mV s^{-1}. Arrow e) shows the potential $E=-0.7$ V that is applied on the electrodes upon the DNA-detection according to Figure 2.

potential for the reduction of O_2 is substantially lower. These results clearly indicate that the intercalated **3** electrocatalyzes the reduction of O_2. It is known that quinones catalyze the electrochemical reduction of O_2 to H_2O_2.[17] A rotating-disc ring-electrode experiment[18] was performed using a Au-disc-electrode modified with the **1**/**2**-assembly and intercalated **3** for the reduction of O_2, and a bare Au-ring electrode was used for the electrochemical detection of the product generated on the disc-electrode. This experiment reveals that the **3**-electrocatalyzed reduction of O_2 (at $E=-0.7$ V) generates H_2O_2 with a yield corresponding to about 90%. It should be noted, however, that a rotating Au-disc electrode modified with **1** and treated with **3** (5.2×10^{-5} M) followed by rinsing, also produces H_2O_2 (detected at the Au-ring electrode) with a current yield that corresponds to about 8% (See Supporting Information). That is, in the presence of **1**-functionalized electrode and in the absence of **3**, the non-catalyzed reduction of O_2 generates mainly H_2O. These results indicate that at a constant potential of -0.7 V the **1**-functionalized electrode will not generate substantial amounts of H_2O_2 by the direct electrochemical reduction of O_2, but the ds-DNA assembly with intercalated **3** will effectively yield H_2O_2 at this potential. Thus, the electrically generated biochemiluminescence, or the electrically driven biocatalyzed precipitation of **5**, would occur mainly in the presence of the ds-DNA system with intercalated **3**.

Figure 4, curve a, shows the emitted light intensity by the system that includes the **1**/**2** double-stranded assembly with

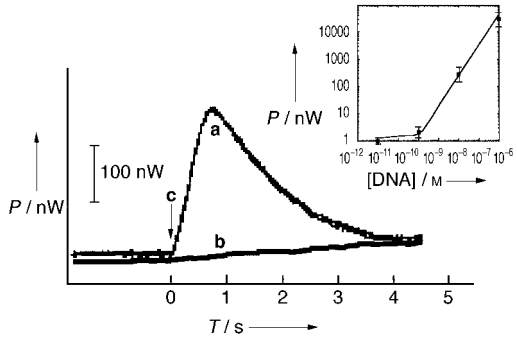

Figure 4. Emitted light intensities from the Au-electrode functionalized with: a) The **1**/**2**-monolayer and intercalated **3**. b) The **1**/**2a**-monolayer treated with **3**. The complementary DNA **2** and mutant DNA **2a** were used with a bulk concentration of 1×10^{-6} M. The light emission was induced by the application of $E=-0.7$ V on the modified electrode in an electrolyte solution composed of 0.1 M phosphate buffer, pH 7.0, that includes luminol (1×10^{-6} M) and HRP (1 mg mL^{-1}) in the presence of O_2. Arrow c) shows the time when the potential was applied on the electrode. Inset: Calibration plot corresponding to the emitted light intensity versus the bulk concentration of **2** analyzed according to Figure 2A. (Each of the error bars originate from four independent functionalized electrodes).

the intercalated **3** on the electrode. A peak-shaped light-emission curve was observed as a result of the rapid depletion of oxygen in the vicinity of the electrode, by its electrocatalytic reduction. Indeed, to observe reproducible light intensities upon applying a sequence of potential pulses (from 0.0 V to -0.7 V and back to 0.0 V), it is necessary to wait for 30 sec between the pulses to allow the equilibration of oxygen at the electrode surface. Figure 4, curve b, shows the intensity of the light emitted by the **1**-functionalized electrode that was interacted with the mutant (**2a**) and further treated with **3**. Only small, slowly increasing, light emission, which corresponds to the non-catalytic formation of H_2O_2 is observed, and indicates that no hybridization with the mutant occurred, and no intercalation of **3** into the monolayer took place. Further control experiments revealed that very little light emission is detected by the **1**/**2** double-stranded monolayer in the absence of **3**. These results clearly indicate that the main biochemiluminescence originates from the reduction of O_2, electrocatalyzed by the intercalated **3** which yields H_2O_2 as the reactive compound for the generation of the emitted light, Figure 2A. The concentration of **1**/**2**, and as a result the amount of intercalated **3** and electrocatalytically generated H_2O_2, and the intensity of emitted light, would be controlled by the bulk concentration of DNA **2**. Figure 4, inset, shows the emitted light intensities at different bulk concentrations of **2**. The detection limit of the analyte **2** by the system is around 2×10^{-11} M.

  0044-8249/02/4118-3400 $ 20.00+.50/0 *Angew. Chem. Int. Ed.* **2002**, *41*, No. 18

The amplified detection of DNA according to Figure 2B, where the **3**-induced biocatalyzed precipitation of **5** is examined by using Faradaic impedance spectroscopy, is shown in Figure 5. The interfacial electron-transfer resistance

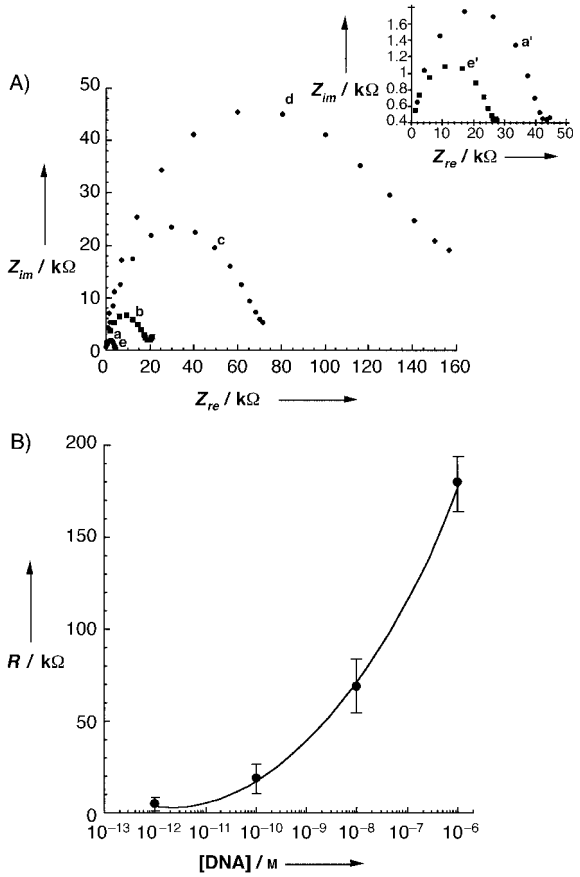

Figure 5. A) Faradaic impedance spectra (Nyquist plots) of the **1**/**2**-DNA assembly with the intercalator **3** after the electrochemically induced (at $E = -0.7$ V) precipitation of **5** for 2 min, upon the analysis of different bulk concentrations of **2**: a) 1×10^{-12} M, b) 1×10^{-10} M, c) 1×10^{-8} M, d) 1×10^{-6} M. Spectrum e) corresponds to the analysis of the mutant DNA (**2a**), 1×10^{-6} M. Inset: Faradaic impedance spectra recorded after 10 min of precipitation of **5** for: a′) **1**/**2**-DNA assembly using 1×10^{-12} M of **2**, e′) **1**/**2a**-DNA assembly using 1×10^{-6} M of **2a**. The Faradaic impedance spectra were recorded in the presence of 10 mM $K_3[Fe(CN)_6]/K_4[Fe(CN)_6]$ (1:1) upon application of a bias potential of $E = 0.175$ V. B) Calibration plot of the electron transfer resistances derived from the Faradaic impedance spectra versus bulk concentration of **2**. The precipitation of **5** was performed for 2 min. (Each of the error bars originate from four independent functionalized electrodes).

of the **1**-functionalized Au-electrode corresponds to $R_{et} = 5$ kΩ (the value was derived from the respective impedance spectrum). The **1**-functionalized electrodes were hybridized with different concentrations of **2** and treated with **3**. The resulting electrodes were subjected to a potential of −0.7 V in the presence of O_2, 4-chloronaphthol (**4**), and HRP, and the precipitation of **5** was allowed to proceed for 2 min. The interfacial electron-transfer resistances, R_{et}, at the modified electrodes that include the precipitated **5** were measured and presented in the form of a Nyquist-plot (Figure 5A). The resulting interfacial R_{et} is controlled by the bulk concentration of the analyte DNA **2**. For example, the interfacial R_{et} resulted upon analyzing **2** at concentrations of 1×10^{-6} M and 1×10^{-10} M are 180 kΩ and 20 kΩ, Figure 5A, curves d and b, respectively. The interfacial R_{et} of the **1**-functionalized-electrodes, upon analyzing **2** at a concentration of 1×10^{-12} M or analyzing the mutant **2a**, at a concentration corresponding to 1×10^{-6} M, are very similar to the **1**-modified electrode, $R_{et} \approx 5$ kΩ, curves a and e, respectively. This result indicates that **2** cannot be sensed at a concentration of 1×10^{-12} M under these experimental conditions, and that the mutant **2a** is fully differentiated from the target DNA **2**. Enhanced sensitivities, however, may be achieved by prolonging the biocatalyzed precipitation process. Figure 5A, inset, shows the interfacial R_{et} resulting from the analysis of **2**, 1×10^{-12} M, and **2a**, 1×10^{-6} M, by stimulating the biocatalyzed precipitation of **5** for a 10 min, curves a′ and e′, respectively. While the precipitation of **5** on the electrodes for 2 min did not enable the sensing of **2**, 1×10^{-12} M, or its differentiation from **2a**, the biocatalyzed precipitation of **5** for 10 min enables the sensing of **2**, $R_{et} =$ 42 kΩ, and its differentiation from the mutant **2a**, $R_{et} = 28$ kΩ. Control experiments reveal that the biocatalyzed precipitation of **5** occurs only if **3** is intercalated into the ds DNA, and provided that the potential of $E = -0.7$ V is applied on the electrode. These results clearly confirm that the biocatalyzed precipitation of **5** is stimulated by the electrocatalyzed reduction of O_2 to H_2O_2 by using doxorubicin (**3**), as an electrocatalyst.

In conclusion, the present study has demonstrated that the intercalation of doxorubicin (**3**), into ds DNA enables the amplified detection of DNA by the doxorubicin-electrocatalyzed reduction of O_2 to H_2O_2. The formation of H_2O_2 is then probed by the generated biochemiluminescence in the presence of luminol/HRP, or by following the changes in the interfacial electron-transfer resistance (R_{et}) resulting from the biocatalyzed precipitation of **5**, by using Faradaic impedance spectroscopy. The detection limits of the target DNA **2** by the electrogenerated biochemiluminescence and biocatalyzed precipitation of the insoluble product are very similar, about 10^{-10} M. This detection limit is comparable to other amplification methods developed in our laboratory[5–7] for short nucleic acids.

Experimental Section

The DNA oligonucleotides **1**, **2**, and **2a**, horseradish peroxidase, HRP, (E.C. 1.11.1.7) and all other chemicals were obtained from Aldrich and Sigma and used as supplied. The Au-coated (50 nm gold layer) glass plate (Analytical-μSystem, Germany) was used as a working electrode (0.3 cm^2 area exposed to the solution). An auxiliary Pt electrode and a quasi-reference Ag electrode were made from wires of 0.5 mm diameter and added to the cell. The quasi-reference electrode was calibrated versus the saturated calomel electrode (SCE) and the potentials are given versus SCE. An open electrochemical cell (230 μL) that includes the modified Au-electrode in a horizontal position and a light detector linked to a fiber optic cable enabled easy light-emission measurements upon application of the appropriate potential to the modified working electrode. The working Au-electrode was treated with a solution of thiolated DNA-primer (**1**; 5×10^{-6} M in 0.3 M phosphate buffer, pH 7.4, 12 h), the electrode was washed with the phosphate buffer, and then the **1**-functionalized Au-surface was treated with 1-mercaptohexanol (1×10^{-3} M in ethanol, 1 h). The resulting monolayer-functionalized electrode was treated with the complementary analyte DNA (**2**; various concentrations in 0.4 M phosphate buffer, pH 7.4, 3 h) to yield the ds-DNA assembly on the electrode surface. The resulting system was further treated with doxorubicin, (**3**; 5.2×10^{-5} M in 0.1M

  0044-8249/02/4118-3401 $ 20.00+.50/0

phosphate buffer, pH 7.4, 30 min). The electrochemical measurements were performed by using an electrochemical impedance analyzer (EG&G, model 1025) and potentiostat (EG&G, model 283) connected to a computer (EG&G Software Power Suite 1.03 and no. 270/250 for impedance and cyclic voltammetry, respectively). All the measurements were performed in 0.1M phosphate buffer solution, pH 7.0, at room temperature. When needed, oxygen was removed from the solution by passing Ar above the cell. The Faradaic impedance measurements were performed in the frequency range of 100 mHz to 50 kHz in the presence of 10 mM $K_3[Fe(CN)_6]/K_4[Fe(CN)_6]$ (1:1 mixture) as a redox probe and upon biasing the working electrode at $E = 0.175$ V. The electrochemically induced biochemiluminescence was measured with a light detector (Laserstat, Ophir) linked to an oscilloscope (Tektronix TDS 220). The light detector was connected to the electrochemical cell by an optical fiber and a potential corresponding to $E = -0.7$ V was applied on the working electrode. The background electrolyte solution was equilibrated with air and included luminol (1×10^{-6}M), and HRP (1 mg mL^{-1}). The electrochemically induced precipitation of the insoluble material (**5**) was performed upon application of a potential that corresponded to $E = -0.7$ V on the working electrode in 0.1M phosphate buffer, pH 7.0. The electrolyte solution was equlibrated with air and included 4-chloro-1-naphthol (**4**; 1×10^{-3}M) and HRP (1 mg mL^{-1}).

Received: January 24, 2002
Revised: April 4, 2002 [Z18576]

[1] a) F. F. Bier, F. Kleinjung, *Fresenius J. Anal. Chem.* **2001**, *371*, 151 – 156; b) E. K. Lobenhofer, P. R. Bushel, C. A. Afshari, H. K. Hamadeh, *Environ. Health Perspect.* **2001**, *109*, 881 – 891; c) K. M. Kurian, C. J. Watson, A. H. Wyllie, *J. Pathol.* **1999**, *187*, 267 – 271.
[2] a) R. F. Service, *Science* **1998**, *282*, 399 – 401; b) M. Ogihara, A. Ray, *Nature* **2000**, *403*, 143 – 144; c) L. M. Wang, O. H. Liu, R. M. Corn, A. E. Condon, L. M. Smith, *J. Am. Chem. Soc.* **2000**, *122*, 7435 – 7440.
[3] a) C. N. Campbell, D. Gal, N. Cristler, C. Banditrat, A. Heller, *Anal. Chem.* **2002**, *74*, 158 – 162; b) T. de Lumley-Woodyear, D. J. Caruana, C. N. Campbell, A. Heller, *Anal. Chem.* **1999**, *71*, 394 – 398.
[4] F. Patolsky, Y. Weizmann, I. Willner, *J. Am. Chem. Soc.*, **2002**, *124*, 770—772..
[5] A. Bardea, F. Patolsky, A. Dagan, I. Willner, *Chem. Commun.* **1999**, 21 – 22.
[6] F. Patolsky, E. Katz, A. Bardea, I. Willner, *Langmuir* **1999**, *15*, 3703 – 3706.
[7] a) F. Patolsky, A. Lichtenstein, I. Willner, *J. Am. Chem. Soc.* **2000**, *122*, 418 – 419; b) F. Patolsky, A. Lichtenstein, I. Willner, *Angew. Chem.* **2000**, *112*, 970 – 973; *Angew. Chem. Int. Ed.* **2000**, *39*, 940 – 943; c) F. Patolsky, A. Lichtenstein, I. Willner, *J. Am. Chem. Soc.* **2001**, *123*, 5194 – 5205.
[8] a) F. Patolsky, K. T. Ranjit, A. Lichtenstein, I. Willner, *Chem. Commun.* **2000**, 1025 – 1026; b) Y. Weizmann, F. Patolsky, I. Willner, *Analyst* **2001**, *126*, 1502 – 1504; c) L. He, M. D. Musick, S. R. Nicewarner, F. G. Salinas, S. J. Benkovic, M. J. Natan, C. D. Keating, *J. Am. Chem. Soc.* **2000**, *122*, 9071 – 9077.
[9] I. Willner, F. Patolsky, J. Wasserman, *Angew. Chem.* **2000**, *113*, 1913 – 1916; *Angew. Chem. Int. Ed.* **2001**, *40*, 1861 – 1864.
[10] a) A. W. Knight, *Trends Anal. Chem.* **1999**, *18*, 47 – 62; b) K. A. Fähnrich, M. Pravda, G. G. Guilbault, *Talanta* **2001**, *54*, 531 – 559.
[11] a) V. C. Tsafack, C. A. Marquette, F. Pizzolato, L. J. Blum, *Biosens. Bioelectron.* **2000**, *15*, 125 – 133; b) C. A. Marquette, L. J. Blum, *Anal. Chim. Acta* **1999**, *381*, 1 – 10; c) B. Leca, L. J. Blum, *Analyst* **2000**, *125*, 789 – 791.
[12] a) X.-H. Xu, H. C. Yang, T. E. Mallouk, A. J. Bard, *J. Am. Chem. Soc.* **1994**, *116*, 8386 – 8387; b) X.-H. Xu, A. J. Bard, *J. Am. Chem. Soc.* **1995**, *117*, 2627 – 2631; c) A. J. Bard, G. Whitesides, US Patent 5,310,687 **1991**; A. J. Bard, G. Whitesides, US Patent 5,221,605 **1990**; A. J. Bard, G. Whitesides, US Patent 5,238,808 **1985**.
[13] G. C. Fiaccabrino, N. F. de Rooij, M. Koudelka-Hep, *Anal. Chim. Acta* **1998**, *359*, 263 – 267.
[14] a) S. M. Zeman, D. R. Phillips, D. M. Crothers, *Proc. Natl. Acad. Sci. USA* **1998**, *95*, 11561 – 11565; b) F. Arcamone, *Doxorubicin: Anticancer Antibiotics*, Academic Press, New York, **1981**; c) M. S. Yang, H. C. M. Yau, H. L. Chan, *Langmuir* **1998**, *14*, 6121 – 6129.
[15] L. Alfonta, A. Bardea, O. Khersonsky, E. Katz, I. Willner, *Biosens. Bioelectron.* **2001**, *16*, 675 – 687.
[16] The surface-coverage of ds DNA was determined according to: A. B. Steel, T. M. Herne, M. J. Tarlov, *Anal. Chem.* **1998**, *70*, 4670 – 4677.
[17] G. S. Calabrese, R. W. Buchanan, M. S. Wrighton, *J. Am. Chem. Soc.* **1983**, *105*, 5594 – 5600.
[18] E. Katz, H.-L. Schmidt, *J. Electroanal. Chem.* **1994**, *368*, 87 – 94.

An Electrochemical Probe of DNA Stacking in an Antisense Oligonucleotide Containing a C3′-*endo*-Locked Sugar**

Elizabeth M. Boon, Jacqueline K. Barton,* Pushpangadan I. Pradeepkumar, Johan Isaksson, Catherine Petit, and Jyoti Chattopadhyaya*

The sensitivity of charge transport chemistry to base stacking[1–5] provides the foundation for applications of DNA charge transport that probe nucleic acid structure, particularly those utilizing electrochemistry experiments on DNA films.[6–13] In these experiments, DNA oligonucleotide duplexes modified with a thiol linker are self-assembled on a gold electrode surface. A redox-active intercalator, such as methylene blue, bound to the close-packed DNA films is electrochemically reduced and the reduced intercalator is used as a catalyst for the reduction of a species diffusing in solution outside of the DNA film (usually ferricyanide). Once re-oxidized by ferricyanide, methylene blue is available for subsequent electrochemical reduction and the catalytic cycle continues.[9,10] The electrochemical reduction of methylene blue takes place via charge transport through the DNA base stack, and thus perturbations in base-pair stacking are repeatedly interrogated in this assay, rendering the electrocatalytic assay exquisitely sensitive to even the smallest disruptions in π stacking. Using this technique, we have detected all single base mismatches as well as several common DNA base damage products.[10] Base-stacking perturbations are also detected within DNA/RNA hybrid duplexes.[12] Furthermore, the electrochemical reduction of DNA intercalators bound to DNA-modified electrodes has been used to monitor DNA–protein interactions.[13] Since this chemistry is extremely sensitive to very small changes in DNA base-pair stacking, we may exploit this assay more generally in probing

[*] Prof. J. K. Barton, E. M. Boon
Division of Chemistry and Chemical Engineering
California Institute of Technology
Pasadena, CA 91125 (USA)
Fax: (+1) 626-577-4976
E-mail: jkbarton@caltech.edu
Prof. J. Chattopadhyaya, P. I. Pradeepkumar, J. Isaksson, Dr. C. Petit
Department of Bioorganic Chemistry
Biomedical Center, University of Uppsala
751 23 Uppsala (Sweden)
Fax: (+46) 18554495
E-mail: jjyoti@boc.uu.se

[**] This work was supported by the National Institutes of Health (GM61077 to J.K.B.), the Swedish Natural Science Research Council (N.F.R.), the Swedish Research Council for Engineering Sciences (T.F.R.), and the Stiftelsen för Strategisk forskning (J.C.).

  0044-8249/02/4118-3402 $ 20.00+.50/0